Transient regimes and crossover for epitaxial surfaces

Citation: Haselwandter, Christoph A., and Dimitri D. Vvedensky. "Transient Regimes and Crossover for Epitaxial Surfaces." Physical Review E 81.2 (2010) : 021606. © 2010 The American Physical Society

As Published: http://dx.doi.org/10.1103/PhysRevE.81.021606

Publisher: American Physical Society

Persistent URL: http://hdl.handle.net/1721.1/64983

Version: Final published version: final published article, as it appeared in a journal, conference proceedings, or other formally published context

Transient regimes and crossover for epitaxial surfaces

Christoph A. Haselwandter*
Department of Physics, Massachusetts Institute of Technology, Cambridge, Massachusetts 02139, USA

Dimitri D. Vvedensky
The Blackett Laboratory, Imperial College London, London SW7 2AZ, United Kingdom
(Received 3 September 2009; published 18 February 2010)

We apply a formalism for deriving stochastic continuum equations associated with lattice models to obtain equations governing the transient regimes of epitaxial growth for various experimental scenarios and growth conditions. The first step of our methodology is the systematic transformation of the lattice model into a regularized stochastic equation of motion that provides initial conditions for differential renormalization-group (RG) equations for the coefficients in the regularized equation. The solutions of the RG equations then yield trajectories that describe the original model from the transient regimes, which are of primary experimental interest, to the eventual crossover to the asymptotically stable fixed point. We first consider regimes defined by the relative magnitude of deposition noise and diffusion noise. If the diffusion noise dominates, then the early stages of growth are described by the Mullins-Herring (MH) equation with conservative noise. This is the classic regime of molecular-beam epitaxy. If the diffusion and deposition noise are of comparable magnitude, the transient equation is the MH equation with nonconservative noise. This behavior has been observed in a recent report on the growth of aluminum on silicone oil surfaces [Z.-N. Fang *et al.*, Thin Solid Films **517**, 3408 (2009)]. Finally, the regime where deposition noise dominates over diffusion noise has been observed in computer simulations, but does not appear to have any direct experimental relevance. For initial conditions that consist of a flat surface, the Villain-Lai-Das Sarma (VLDS) equation with nonconservative noise is not appropriate for any transient regime. If, however, the initial surface is corrugated, the relative magnitudes of terms can be altered to the point where the VLDS equation with *conservative* noise does indeed describe transient growth. This is consistent with the experimental analysis of growth on patterned surfaces [H.-C. Kan *et al.*, Phys. Rev. Lett. **92**, 146101 (2004); T. Tadayyon-Eslami *et al.*, Phys. Rev. Lett. **97**, 126101 (2006)].

DOI: 10.1103/PhysRevE.81.021606 PACS number(s): 81.15.Aa, 05.40.−a, 05.10.Gg

I. INTRODUCTION

In a series of papers [1–5], we have developed a systematic methodology for deriving stochastic continuum equations for lattice models of driven fluctuating interfaces. These models are formulated in terms of stochastic transition rules for the site occupancies on (typically square) lattices. The first step of our methodology is the transformation of these rules into a lattice Langevin equation [1], which is then converted into a regularized stochastic continuum equation [4,5]. With this regularized equation as the initial condition, differential renormalization-group (RG) equations [6,7] are formulated for the changes in the coefficients of the regularized equation under coarse graining. The solutions of the RG equations yield trajectories that describe the original model over a hierarchy of length and time scales, from the initial microscopic description to the asymptotically stable fixed point. The latter behavior provides the statistical mechanical classification of such models based on universality classes [8,9]. Thus, our method yields sequences of continuum equations that describe growth models over expanding length and time scales, while retaining a direct connection to the underlying atomistic transition rules.

Our interest here is in the transient regime for several experimental scenarios, where, for a given model, the regularized continuum description is determined by the growth conditions (temperature and flux) and substrate preparation, such as patterning. The regularized equation determines the initial path traced out by the RG trajectory which, in turn, affects the passage near unstable fixed points before the crossover to the asymptotically stable fixed point [10]. These transients are of direct experimental interest since, apart from buffer layers, typically 100 or so layers of material are deposited either in fundamental growth studies or for further processing. Thus, equations that do not correspond to stable fixed points may nevertheless describe such experiments. Accordingly, by providing an accurate description of the transient regime, our analysis is able to account for a diverse range of experimental observations within a unified framework.

We will focus our attention on models that incorporate basic rules for deposition and diffusion on simple orthogonal lattices. Such models, which typically include random deposition and nearest-neighbor hopping at a rate determined by the nearest-neighbor environment [11–13], have accounted for several fundamental aspects of epitaxial phenomena, including surface diffraction measurements [14,15], submonolayer island statistics at various levels of resolution [16], and multilayer morphologies [16,17]. We have previously shown [3,5] that the asymptotic continuum description of random deposition/diffusion models is the Villain-Lai-Das Sarma (VLDS) equation [18,19] with nonconservative noise.

The outline of this paper is as follows. In Sec. II, we present a dimensionless formulation of the regularized equa-

*Present address: Department of Applied Physics, California Institute of Technology, Pasadena, California 91125, USA.

tion describing random deposition and thermally activated hopping. The differential RG equations for this formulation are summarized in Sec. III. Section IV describes the effects of temperature and flux on the form of the initial regularized equation, while Sec. V examines the RG trajectories from various initial conditions. In Sec. VI, we discuss the interplay between deposition and diffusion noise, and in Sec. VII, we provide a summary and outline some outstanding issues.

II. DIMENSIONLESS FORMULATION

We consider a model with concurrent random deposition and nearest-neighbor hopping on a simple orthogonal lattice. Growth proceeds by deposition of atoms with a flux $F=a_\perp/\tau_0$, where $a_\perp$ is the vertical lattice constant and τ_0^{-1} is the deposition rate. Upon arrival at the substrate, surface adatoms hop to nearest-neighbor sites at the rate

$$\nu = \nu_0 \exp[-\beta(E_S + nE_N)], \tag{1}$$

where $\nu_0 \approx 10^{13}$ s^{-1} is the attempt frequency, $\beta^{-1}=k_BT$, k_B is Boltzmann's constant, T is the substrate temperature, E_S is the contribution to the migration barrier from the substrate, and E_N is the corresponding contribution from each of the n lateral nearest neighbors, where $n=0,1,\ldots,2d$, for a d-dimensional substrate. The height $h(\mathbf{x},t)$ of the fluctuating interface at position $\mathbf{x}$ on the substrate at time t produced by this model is governed by the equation [3]

$$\frac{\partial h}{\partial t} = -\nu_4\nabla^4 h + \lambda_{22}\nabla^2(\nabla h)^2 + F + \xi, \tag{2}$$

in which

$$\nu_4 = \frac{a_\parallel^4}{a_\perp^2}\frac{D_S}{2d}B\gamma(1-A\gamma)^{2d-1}, \tag{3}$$

$$\lambda_{22} = -\frac{a_\parallel^4}{a_\perp^3}\frac{D_S}{2d}\gamma(1-A\gamma)^{2d-2}[B^2\gamma + 2C(1-A\gamma)], \tag{4}$$

where $a_\parallel$ is the horizontal lattice constant (with $a_\parallel=a_\perp$ corresponding to a cubic lattice), $D_S=a_\perp^2\nu_0 e^{-\beta E_S}$ is the height diffusion constant, and $\gamma=1-e^{-\beta E_N}$ so that $0\le\gamma\le 1$. The Gaussian noise $\xi(\mathbf{x},t)$ has mean zero and covariance

$$\langle \xi(\mathbf{x},t)\xi(\mathbf{x}',t')\rangle = 2\mathcal{D}\delta^d(\mathbf{x}-\mathbf{x}')\delta(t-t'), \tag{5}$$

with $\mathcal{D}=D_0-D_2\nabla^2$, and

$$D_0 = a_\parallel^d\frac{a_\perp^2}{2\tau_0}, \quad D_2 = a_\parallel^{d+2}\frac{D_S}{2d}(1-A\gamma)^{2d}. \tag{6}$$

We have $A=0.5$, $B=0.006$, and $C=-3\times10^{-7}$ for the representative value $\delta=0.01$ of the regularization parameter [4,5], which is chosen small enough so that the coefficients of higher-order terms take much smaller magnitudes than those retained in Eq. (2).

By transforming the time, space, and height variables to corresponding dimensionless quantities

$$\bar{t} = \frac{t}{\tau_0}, \quad \bar{\mathbf{x}} = \frac{\mathbf{x}}{a_\parallel}, \quad \bar{h} = \frac{h}{a_\perp}, \tag{7}$$

we obtain the alternative form of Eq. (2)

$$\frac{\partial \bar{h}}{\partial \bar{t}} = -\bar{\nu}_4\bar{\nabla}^4\bar{h} + \bar{\lambda}_{22}\bar{\nabla}^2(\bar{\nabla}\bar{h})^2 + 1 + \bar{\xi}, \tag{8}$$

with dimensionless coefficients

$$\bar{\nu}_4 = \frac{R}{2d}B\gamma(1-A\gamma)^{2d-1}, \tag{9}$$

$$\bar{\lambda}_{22} = -\frac{R}{2d}\gamma(1-A\gamma)^{2d-2}[B^2\gamma + 2C(1-A\gamma)], \tag{10}$$

where $R=\tau_0\nu_0 e^{-\beta E_S}$,

$$\langle \bar{\xi}(\bar{\mathbf{x}},\bar{t})\bar{\xi}(\bar{\mathbf{x}}',\bar{t}')\rangle = 2\bar{\mathcal{D}}\delta^d(\bar{\mathbf{x}}-\bar{\mathbf{x}}')\delta(\bar{t}-\bar{t}'), \tag{11}$$

$\bar{\mathcal{D}}=\bar{D}_0-\bar{D}_2\bar{\nabla}^2$, and

$$\bar{D}_0 = \frac{1}{2}, \quad \bar{D}_2 = \frac{R}{2d}(1-A\gamma)^{2d}. \tag{12}$$

The quantity R is a dimensionless measure of the relative magnitudes of the diffusion constant and the deposition flux,

$$\frac{D_S}{F} = \frac{a_\perp^2\nu_0 e^{-\beta E_S}}{a_\perp/\tau_0} = a_\perp R, \tag{13}$$

which characterizes the typical lateral feature size of the surface morphology [20]. Note that the coefficients $\bar{\nu}_4$ and $\bar{\lambda}_{22}$ are determined by the product of R and the function $\gamma=\gamma(E_N,T)$, which controls the importance of detachment events, while $\bar{D}_0$ does not depend on R or γ. In particular, from Eqs. (9)–(12), we see that the ratio $\bar{\nu}_4/\bar{\lambda}_{22}$ is determined only by γ but $\bar{D}_2/\bar{D}_2$ is determined by both R and γ, which we will return to in Sec. IV.

One of the central points of our analysis is that all of the quantities that enter the coefficients of the regularized microscopic description depend on the parameters of the lattice model, the regularization parameters that determine the extent of initial coarse graining, and the growth parameters (temperature and flux). Thus, at each point of the RG trajectory, the coefficients have values determined by their microscopic values, which establishes a direct relation to the atomistic theory. Moreover, as we will discuss in Sec. V, substrate preparation can also affect the form of the regularized equation through variations in the magnitudes of various derivatives.

III. RENORMALIZATION-GROUP EQUATIONS

The coefficients in the dimensionless Eq. (8) renormalize under the scale changes $\bar{\mathbf{x}}\to e^{\ell}\bar{\mathbf{x}}$, $\bar{t}\to e^{z\ell}\bar{t}$, and $\bar{h}\to e^{\alpha\ell}\bar{h}$ to one-loop order as [3,19,21]

$$\frac{d\bar{\nu}_4}{d\ell} = \left(z-4-\frac{K_d}{d}\frac{\bar{D}_s\bar{\lambda}_{22}^2\Lambda^{d-4}}{\bar{\nu}_4^3}\right)\bar{\nu}_4, \tag{14}$$

$$\frac{d\bar{\lambda}_{22}}{d\ell} = (z-4+\alpha)\bar{\lambda}_{22}, \tag{15}$$

$$\frac{d\bar{D}_0}{d\ell} = (z - d - 2\alpha)\bar{D}_0, \tag{16}$$

$$\frac{d\bar{D}_2}{d\ell} = (z - d - 2\alpha - 2)\bar{D}_2, \tag{17}$$

$$\frac{d\bar{D}_4}{d\ell} = \left(z - d - 2\alpha - 4 + K_d \frac{\bar{\lambda}_{22}^2 \bar{D}^2 \Lambda^{d-8}}{\bar{\nu}_4^3 \bar{D}_4}\right)\bar{D}_4, \tag{18}$$

where $K_d = S_d/(2\pi)^d$, $S_d = 2\pi^{d/2}/\Gamma(\frac{1}{2}d)$ is the surface area of a d-dimensional unit sphere,

$$\bar{D}_s = \sum_{i=0}^{2} (d - 6 + 2i)\bar{D}_{2i}\Lambda^{2i}, \tag{19}$$

$\bar{D} = \bar{D}_0 + \bar{D}_2\Lambda^2 + \bar{D}_4\Lambda^4$, and $\Lambda = 2\pi$ is the momentum cutoff in our dimensionless formulation of the model.

The exponents z and α take constant values at a fixed point of the RG and thereby define the self-affine surface morphology associated with that fixed point (see Appendix). For general microscopic growth parameters, however, the values of the coefficients in Eq. (8) differ from their (asymptotic) fixed point values. In this case, the values of the exponents z and α can change along the trajectory. To study the crossover behavior of our model, we therefore transform the RG equations (14)–(18) into a form that does not explicitly involve the scaling exponents. This is achieved by introducing the quantities

$$r = \frac{\bar{D}_0 \bar{\lambda}_{22}^2}{\bar{\nu}_4^3}\Lambda^{d-4}, \quad \Gamma_2 = \frac{\bar{D}_2}{\bar{D}_0}\Lambda^2, \quad \Gamma_4 = \frac{\bar{D}_4}{\bar{D}_0}\Lambda^4, \tag{20}$$

in terms of which the RG equations (14)–(18) become

$$\frac{dr}{d\ell} = \left(4 - d + \frac{3K_d}{d} r\Gamma\right) r, \tag{21}$$

$$\frac{d\Gamma_2}{d\ell} = -2\Gamma_2, \tag{22}$$

$$\frac{d\Gamma_4}{d\ell} = -4\Gamma_4 + K_d r(1 + \Gamma_2 + \Gamma_4)^2, \tag{23}$$

where

$$\Gamma = d - 6 + (d - 4)\Gamma_2 + (d - 2)\Gamma_4. \tag{24}$$

The relative powers of the quantities in Eq. (20) are fixed by the requirement that the transformed RG equations must not depend on the scaling exponents.

The fixed points associated with Eqs. (21)–(23) are the Mullins-Herring (MH) fixed point,

$$(r^*, \Gamma_2^*, \Gamma_4^*) = (0,0,0), \tag{25}$$

and two fixed points VLDS$^{\pm}$,

$$(r^*, \Gamma_2^*, \Gamma_4^*)^{\pm} = \left(\frac{d(4-d)}{3K_d[6 - d + (2-d)\Gamma_4^*]}, 0, \frac{-36 + 10d - d^2 \pm 2\sqrt{3}(108 - 52d + 7d^2)^{1/2}}{24 - 16d + d^2}\right), \tag{26}$$

where Γ_4^* in the expression for r^* refers to the value of Γ_4 at the VLDS$^{\pm}$ fixed point.

The MH fixed point is unstable for $d < 4$ but stable for $d > 4$. The VLDS$^-$ fixed point is always unstable, while the VLDS$^+$ fixed point is stable for $d < 4$, but unstable for $d > 4$. Thus, for the physically relevant cases $d = 1$ and $d = 2$ the transformed RG equations (21)–(23) imply [22] that the asymptotic equation describing random deposition-surface diffusion models takes the form of the VLDS equation,

$$\frac{\partial \bar{h}}{\partial \bar{t}} = -\bar{\nu}\bar{\nabla}^4\bar{h} + \bar{\lambda}\bar{\nabla}^2(\bar{\nabla}\bar{h})^2 + \bar{\xi}, \tag{27}$$

where the Gaussian noise $\bar{\xi}(\bar{\mathbf{x}}, \bar{t})$ has mean zero and the covariance in Eq. (11) with $\bar{\mathcal{D}} = \bar{D}_0$, and the relative magnitudes of the coefficients are fixed by Eq. (26) (see Appendix).

Depending on the growth conditions, the transient behavior of our system can be characterized by unstable fixed points of the RG such as the MH fixed point. The MH fixed point is approached asymptotically only in the subspace with $\bar{\lambda}_{22} = 0$ and implies an equation of the form [23,24]

$$\frac{\partial \bar{h}}{\partial \bar{t}} = -\bar{\nu}\bar{\nabla}^4\bar{h} + \bar{\xi}, \tag{28}$$

with $\bar{\mathcal{D}} = \bar{D}_0$.

In the limit of the deposition flux going to zero, we have $D_0 \to 0$ in Eq. (2). In order to analyze the subspace corresponding to $F \to 0$, it is therefore necessary to use modified versions of the transformed variables in Eq. (20). In this case, we consider $\bar{D}_2$ rather than $\bar{D}_0$ as a reference quantity for the relative contributions to the noise strength. One finds, following analogous steps as above, for $d < 4$, a stable fixed point of the RG corresponding to the conserved VLDS (cVLDS) equation [25], Eq. (27) with $\bar{\mathcal{D}} = -\bar{D}_2\bar{\nabla}^2$, and an unstable fixed point corresponding to the conserved MH (cMH) equation, Eq. (28) with $\bar{\mathcal{D}} = -\bar{D}_2\bar{\nabla}^2$. A distinct set of scaling exponents is associated with each of these fixed points.

IV. EXPLORING PARAMETER SPACE

The crossover behavior of Eq. (2) is determined by the microscopic values of the transformed variables r and Γ_2. From Eqs. (9)–(12), one finds

$$r = \frac{(2\pi)^{d-4} d[B^2\gamma + 2C(1-A\gamma)]^2}{\gamma(1-A\gamma)^{2d+1}B^3} R^{-1} \equiv \mathcal{K}_1 R^{-1}, \quad (29)$$

$$\Gamma_2 = \frac{4\pi^2(1-A\gamma)^{2d}}{d} R \equiv \mathcal{K}_2 R, \quad (30)$$

where we have implicitly defined the quantities

$$\mathcal{K}_{1,2} = \mathcal{K}_{1,2}(E_N, T, d, \delta) \quad (31)$$

characterizing the attachment and detachment kinetics of adatoms at edge and kink sites.

For $\gamma \to 0$ (or $E_N \to 0$), $\mathcal{K}_1$ diverges as $1/\gamma$. However,

$$\mathcal{K}_1 < 10^{-2} \quad \text{for} \quad 10^{-5} \leq \gamma \leq 1, \quad (32)$$

with $d=1,2$. For $T<2000$ K, the above range of γ translates to $E_N > 10^{-5}$ eV, which encompasses a much wider range of possible growth parameters than the typical values [14,20,29] $E_N \approx 0.1-1$ eV with $T \approx 300-1000$ K. Thus, although $\mathcal{K}_1$ is a function of E_N, we always have $\mathcal{K}_1 \ll 1$ for physically relevant parameter ranges. Similarly, we have $1 < \mathcal{K}_2 < 20$.

Based on the foregoing considerations, we find

$$r < 10^{-2} R^{-1} \quad \text{and} \quad \Gamma_2 \gtrapprox R. \quad (33)$$

Depending on the value of R, we can therefore distinguish between three regimes.

(i) $R \gg 1$ (with the typical range $R \approx 10^5 - 10^7$). In this case, diffusion noise dominates over deposition noise and the initial behavior is governed by the cMH fixed point. Comparing the microscopic magnitudes of the various coefficients in the dimensionless Eq. (8), one indeed finds $\bar{\nu}_4/\bar{\lambda}_{22} \approx 10^2$ and $\bar{D}_0/\bar{D}_2 \ll 1$. This is the classic regime of molecular-beam epitaxy (MBE), where, for example, the deposition noise can be neglected altogether with no apparent detrimental effect on the distribution of island sizes [26].

(ii) $R \approx 1$ (with the typical range $R \approx 10^{-1} - 10$). Diffusion noise is now almost completely suppressed, even at microscopic scales. Again, we find $\bar{\nu}_4/\bar{\lambda}_{22} \approx 10^2$ but now $\bar{D}_0/\bar{D}_2 \approx 1$, which means that the early stages of growth are described by the MH equation. This behavior has been observed in recent work on the growth of aluminum on silicone oil surfaces [27,28].

(iii) $R \ll 1$ (with the typical range $R \approx 10^{-7} - 10^{-5}$). The effective coupling r takes an appreciable magnitude even at microscopic scales. However, the three coefficients $\bar{\nu}_4$, $\bar{\lambda}_{22}$, and $\bar{D}_2$ are all proportional to $R \ll \bar{D}_0$, which means that the initial stages of growth are dominated by shot noise. This behavior has been observed in computer simulations [3,30] of the random deposition-surface diffusion model for the parameter ranges implied by our analysis.

Thus, we find that the attachment/detachment kinetics to steps are all but irrelevant during the early stages of growth on an initially flat surface (see, however, Sec. V C), i.e., the quantities $\mathcal{K}_1$ and $\mathcal{K}_2$ do not influence the early stages of morphological evolution, and the term $\nabla^2(\nabla h)^2$ can be neglected in this regime. This provides a direct confirmation of the long-standing phenomenological argument [19] that the term $\nabla^2(\nabla h)^2$ describes the attachment and detachment of adatoms at kink sites. Moreover, note that the cVLDS equation does not govern the initial surface properties for *any* values of the growth parameters (again provided that the initial surface morphology is flat).

V. RENORMALIZATION-GROUP TRAJECTORIES

The sequences of effective continuum equations that govern homoepitaxial growth with thermal diffusion across length and time scales are obtained by solving the transformed RG equations (21)–(23) with the initial conditions in Eqs. (8)–(12) that describe the system at atomistic scales. We have shown previously [3] that the resulting RG trajectories are in excellent agreement with all available computer simulations of this model for a range of growth parameters.

A. Effect of growth condition

Figure 1(a) shows the RG trajectory corresponding to the experimental conditions used in Ref. [28], where a crossover from MH to VLDS behavior was observed after the deposition of approximately 40 monolayers of material. The RG trajectory in Fig. 1(a) is calculated using the same growth parameters as in Ref. [28]. In particular, the growth experiments in Ref. [28] were carried out at room temperature ($T \approx 300$ K) at a growth rate $F=0.02$ nm/s. Taking $a_\perp$ to be the atomic diameter of aluminum, which is approximately 0.27 nm [31], we obtain $\tau_0 = 13.5$ s. As shown in Fig. 1(a), a rapid crossover from the MH fixed point to the VLDS$^+$ fixed point is obtained with a value $E_S=0.9$ eV for the contribution to the hopping barrier coming from the substrate. Superimposed on the RG trajectory are points separated by a logarithmic scale of $\Delta\ell = 1/3$. As shown in Fig. 1(b), our analysis indicates that an increase in the substrate temperature used in Ref. [28] would lead to an additional crossover from the cMH fixed point to the MH fixed point prior to the eventual crossover to the VLDS$^+$ fixed point.

In Sec. IV, we found that the attachment/detachment kinetics, parameterized by the quantity E_N in our model, are all but irrelevant for the initial surface evolution. As demonstrated by Figs. 1(c) and 1(d), this behavior persists along the RG trajectory, with the transient behavior of homoepitaxial growth with thermal diffusion showing a relatively small dependence on E_N as compared to the dependence on T (or E_S) shown in Figs. 1(a) and 1(b). Note, however, that the eventual crossover to the asymptotic behavior of the system, which is governed by the VLDS equation, crucially relies on $E_N > 0$.

The behavior of homoepitaxial growth with thermal diffusion is summarized in Fig. 2. For $R \ll 1$, the initial stages of growth are dominated by random deposition, which is followed by a crossover to the VLDS$^+$ fixed point with only a small deflection toward the MH fixed point. With $R \approx 1$, the

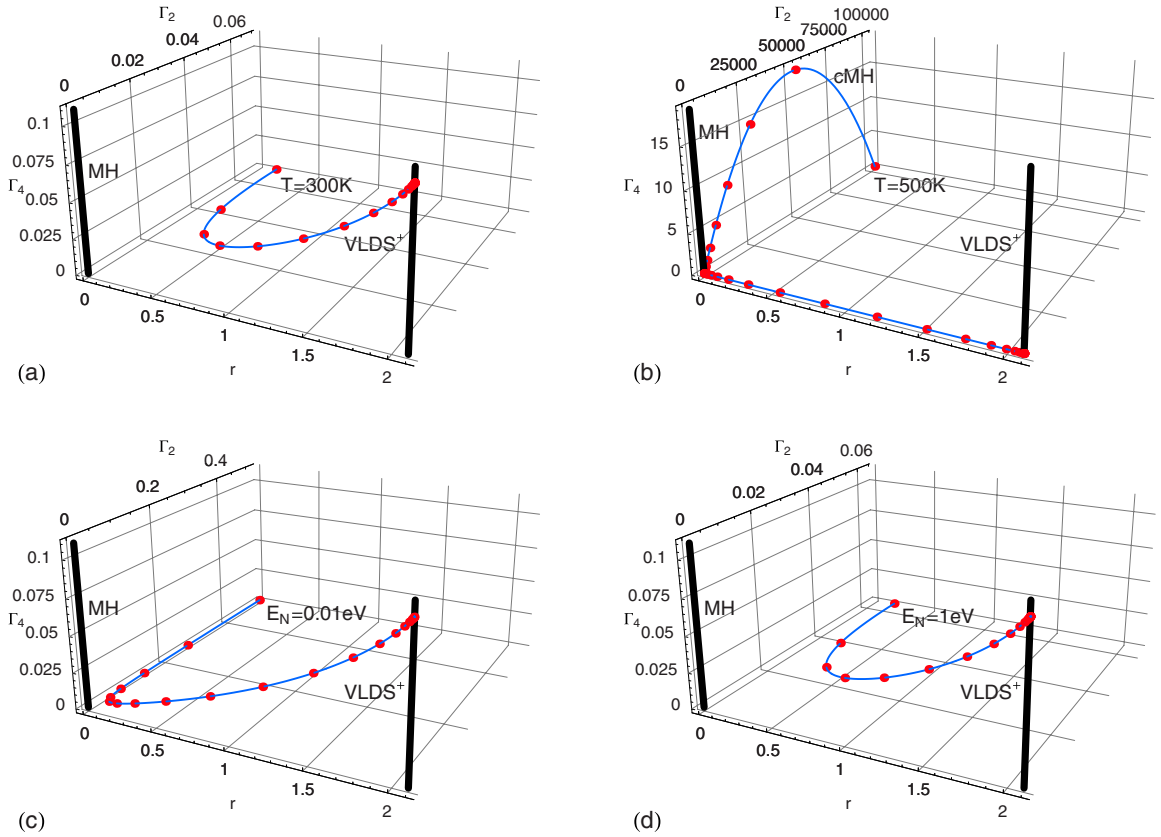

FIG. 1. (Color online) RG trajectories of the random deposition-surface diffusion model obtained from Eqs. (21)–(23) with the initial conditions in Eqs. (8)–(12) for $d=2$ using the parameter values $E_S=0.9$ eV, $\nu_0=5\times10^{12}$ s^{-1}, and $\tau_0=13.5$ s with (a) $E_N=0.1$ eV and the substrate temperature $T=300$ K used in the experiments in Refs. [27,28], (b) $E_N=0.1$ eV and $T=500$ K, (c) $E_N=0.01$ eV and $T=300$ K, and (d) $E_N=1$ eV and $T=300$ K. In all plots, the RG flow is directed toward the VLDS$^+$ fixed point, and superimposed on the RG trajectories are points separated by a logarithmic scale of $\Delta\ell=1/3$.

initial behavior is dominated by the MH fixed point prior to a crossover to the VLDS$^+$ fixed point. If, however, $R\gg1$, the initial behavior is very well described by the cMH equation. This is followed by a pronounced transient regime described by the MH equation before the eventual crossover to the VLDS$^+$ fixed point.

B. Effect of initial coarse graining

In our analysis of homoepitaxial growth with thermal diffusion, we have assumed that $\delta<\delta'\approx0.02$, such that the leading-order Eq. (2) is obtained and higher-order terms can be safely neglected. Our estimates in Eq. (33) and the resulting investigation of parameter space relied on this assumption. It is therefore legitimate to ask what would happen if $\delta>\delta'$, in which case we could have $\mathcal{K}_1\gg1$ at microscopic scales. As shown in Fig. 3, the RG flow of homoepitaxial growth with thermal diffusion is very different for $\delta<\delta'$ and $\delta>\delta'$. In particular, with $\delta>\delta'$, there is no crossover from MH to VLDS$^+$ behavior for $T=670$ K and the growth parameters in Ref. [30], while for $T=700$ K, the RG trajectory takes the system away from the VLDS$^+$ fixed point [see Fig. 3(a)]. These trajectories are in blatant disagreement with the computer simulations carried out for these growth parameters in Ref. [30], while the corresponding RG trajectories obtained for $\delta<\delta'$ [see Fig. 3(b)] are in excellent agreement with simulations. We therefore conclude that, as expected on the basis of the derivation [3–5] of the leading-order Eq. (2), the regime $\delta<\delta'$ is physically relevant while the regime $\delta>\delta'$ is not.

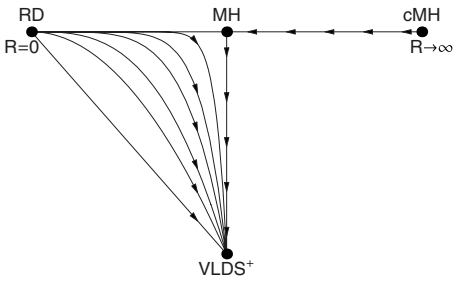

FIG. 2. Schematic representation of the RG flow of the random deposition-surface diffusion model.

C. Patterned substrates

According to the above analysis, the cVLDS fixed point does not describe the dynamics of homoepitaxial growth with surface diffusion for any range of growth parameters or length and time scales. This conclusion, however, only trans-

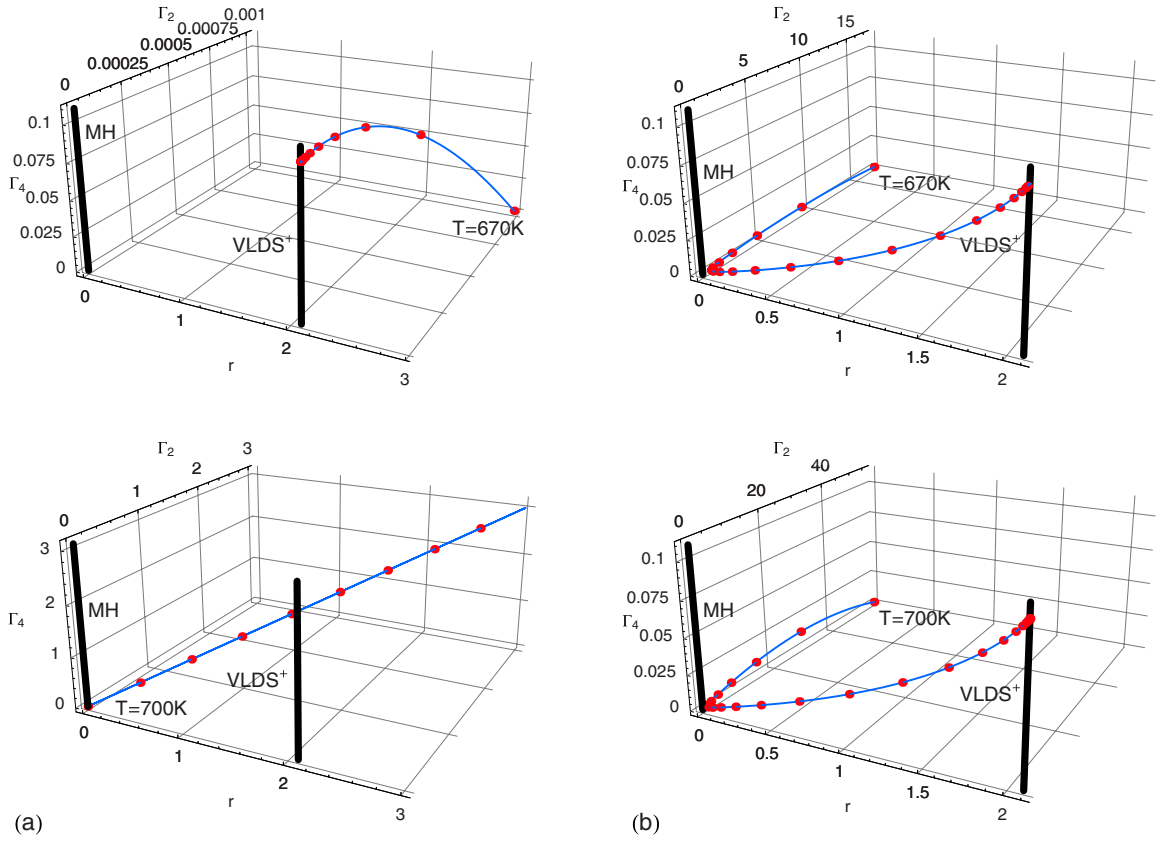

FIG. 3. (Color online) RG trajectories of the random deposition-surface diffusion model obtained from Eqs. (21)–(23) with the initial conditions in Eqs. (8)–(12) for $d=2$ using the parameter values [30] $\tau_0=2$ s, $\nu_0=5\times10^{12}$ s^{-1}, $E_S=1.58$ eV, and $E_N=0.24$ eV for the indicated temperatures with (a) $\delta=10$ and (b) $\delta=0.01$. Superimposed on the RG trajectories are points separated by a logarithmic scale of $\Delta\ell=1/3$. In the upper panel of (a) and the upper and lower panels of (b), the RG flow is directed toward the VLDS$^+$ fixed point, whereas in the lower panel of (a), the RG flow takes the system away from the VLDS$^+$ fixed point.

lates into the statement that the cVLDS equation does not describe the evolution of the surface profile for any regime of homoepitaxial growth if the initial surface morphology is flat. In particular, for corrugated surface morphologies the term $\lambda_{22}\nabla^2(\nabla h)^2$ can dominate over the term $\nu_4\nabla^4 h$ at atomistic scales. Such behavior has indeed been observed in experiments [32–34]. Assuming, for simplicity, that the corrugation of the substrate takes the form

$$h_0(x) = A_0 \cos(\lambda_0 x), \tag{34}$$

one finds that

$$\frac{\bar{\nu}_4}{\bar{\lambda}_{22}} \approx 10^2 \frac{1}{2\bar{A}_0} \approx 1, \tag{35}$$

for $\bar{A}_0=A_0/a_\perp$ and the value $A_0\approx 25$ nm$\approx 50a_\perp$ used in Refs. [32–34], while

$$\frac{\bar{D}_2}{\bar{D}_0} \approx R \gg 1 \tag{36}$$

for the typical MBE growth conditions employed in Refs. [32–34]. Thus, we find that for the growth conditions used in Refs. [32–34] the initial stages of surface evolution are indeed governed by the cVLDS equation.

VI. DEPOSITION VERSUS DIFFUSION NOISE

As seen above, deposition noise asymptotically dominates over diffusion noise for homoepitaxial growth with thermal diffusion because

$$\frac{d\Gamma_2}{d\ell} = -2\Gamma_2. \tag{37}$$

This RG equation for the transformed variable

$$\Gamma_2 = \frac{\Lambda^2 \bar{D}_2}{\bar{D}_0} = \frac{\Lambda^2 a_\parallel^{-2} D_2}{D_0} \tag{38}$$

is exact to any number of loops in the RG calculation and, moreover, does not rely on an *a priori* assumption that the scaling relation

$$z - d - 2\alpha = 0 \tag{39}$$

is satisfied. Indeed, on the basis of the RG analysis, the above scaling relation is satisfied at particular fixed points of the RG, such as the MH and VLDS$^\pm$ fixed points, while it is not satisfied at other fixed points, such as the Kardar-Parisi-Zhang (KPZ) fixed point or the cMH fixed point (see Appendix).

The solution of Eq. (37) is given by

$$\Gamma_2(\ell) = \Gamma_2(\ell = 0)e^{-2\ell}. \tag{40}$$

In the standard MBE regime, we have $R \gg 1$, and, hence, $\Gamma_2(\ell=0) \gg 1$ according to Eq. (33). The degree of coarse graining at which deposition noise starts to dominate over deposition noise is given by $\Gamma_2(\ell) \approx 1$. Thus, using Eq. (40) and noting that scale changes proceed according to $\mathbf{x} \to e^{\ell}\mathbf{x}$ with $\ell=0$ corresponding to a spatial scale $a_{\parallel}/\Lambda$, we find a characteristic length

$$l_c = [\Gamma_2(\ell = 0)]^{1/2} \frac{a_{\parallel}}{\Lambda} \tag{41}$$

beyond which diffusion noise can be safely neglected.

On a more phenomenological level, the above conclusions can also be understood directly on the basis of Eq. (2) by noting that deposition noise is uncorrelated whereas diffusion noise is correlated. The correlations in the diffusion noise have their origin in the random nature of adatom hopping, which means that an "upward" fluctuation at a given lattice site implies a "downward" fluctuation at a nearby site, and vice versa. One therefore (naively) expects that diffusion noise can dominate over deposition noise only up to some spatial scale set by the stochastic part of the diffusion process (which is the stochastic analog of the diffusion length). By dimensional analysis, we therefore find the scale

$$\tilde{l}_c = \left(\frac{D_2}{D_0}\right)^{1/2}, \tag{42}$$

where D_0 and D_2 are the microscopic strengths of deposition and diffusion noise corresponding to $\ell=0$. Thus, we evidently have $\tilde{l}_c = l_c$.

For parameter values corresponding to the experiments in Refs. [27,28] and the RG trajectories in Figs. 1(a) and 1(b), we find $l_c \approx 0.04\ a_{\parallel}$ with $T=300$ K, but $l_c \approx 40\ a_{\parallel}$ with $T=500$ K, respectively. The irrelevance of diffusion noise for $T=300$ K implied by our atomistic model is in agreement with the experiments in Refs. [27,28]. As a *caveat*, we note, however, that our phenomenological argument for the asymptotic irrelevance of diffusion noise only applies because neither D_0 nor D_2 are coupled to other coefficients under the RG. For instance, in the case of nonconserved growth, it has been shown [35] that correlated noise with sufficiently long-lived power-law correlations can dominate asymptotically over deposition noise.

VII. SUMMARY AND CONCLUSIONS

We have shown how our previously developed methodology for deriving regularized stochastic continuum equations, in conjunction with the RG, can account for much of the transient behavior seen in deposition/diffusion systems. This complements our earlier work, which focused on the entire trajectory, where we were able to reproduce complex crossover sequences seen in simulations of several models. In this paper, we first considered regimes delineated by the relative magnitudes of the diffusion noise and the deposition noise. If the diffusion noise dominates, then the early stages of growth are described by the cMH equation. This is the regime in which experiments on MBE are typically carried out.

If the diffusion and deposition noise are of comparable magnitude, the transient equation is the MH equation. This behavior has been observed in recent experiments of aluminum growing on silicone oil surfaces [27,28]. Since the flux and temperature are usually known with reasonable accuracy, we can use the type of analysis described here to place bounds on the values of model parameters, in particular the adatom hopping barrier E_S, once a particular transient behavior has been observed. Finally, the regime where deposition noise dominates over diffusion noise has been observed in computer simulations, but does not appear to have any direct experimental relevance. If the temperature is too low to allow activated hopping, short-range nondiffusive relaxation mechanisms (e.g., funneling [16]) can come to play a crucial role in determining the surface morphology [2,4,5].

Previous work [3] has shown that the fixed point of the deposition/diffusion models we consider here is always the VLDS equation. For an initially flat surface and any physically reasonable growth conditions, this equation is not appropriate for any transient regime. Indeed, under typical growth conditions of MBE, the initial behavior is governed by the cMH equation, followed by a crossover to the MH and VLDS equations, respectively, while for low enough temperatures the initial behavior is governed by random deposition, followed by a crossover to the VLDS equation with, generally, only a "weak" MH regime. If, however, the initial surface is corrugated, the relative magnitudes of terms can be altered to the point where the VLDS equation with *conservative* noise does indeed describe transient growth. This agrees with the analysis of experimental data for growth on patterned surfaces [32–34].

Although we have used our methodology to account for a wide range of simulational and experimental data, which together provide a substantial level of confidence in our procedure, there are several extensions of our work that remain to be carried out. We have considered the regularized equation for corrugated surfaces, but have not calculated RG trajectories to determine the crossover sequence. Taking a more general view, we can imagine a substrate that is initially rough. Some aspects of this have been addressed in the literature [36,37], but a systematic approach along the lines we have described in previous work has yet to be advanced. Moreover, recent studies [38,39] have considered thermal relaxation in porous thin films not subject to the solid-on-solid constraint. Such systems are amenable to a similar approach as described here for the derivation of microscopic and coarse-grained values of the coefficients in the governing equation as a function of the growth conditions.

ACKNOWLEDGMENT

C.A.H. was supported at MIT by the Austrian Science Fund.

APPENDIX: SCALING AND CROSSOVER

For simplicity, consider the classic description of fluctuating interfaces provided by the KPZ equation [40]

$$\frac{\partial h}{\partial t} = \nu \nabla^2 h + \frac{\lambda}{2}(\nabla h)^2 + \xi, \tag{A1}$$

in which the Gaussian noise $\xi(\mathbf{x},t)$ has mean zero and covariance

$$\langle \xi(\mathbf{x},t)\xi(\mathbf{x}',t')\rangle = 2D\delta^d(\mathbf{x}-\mathbf{x}')\delta(t-t'). \tag{A2}$$

Under RG transformations, one finds [40] a flow equation for the effective coupling constant $\bar{\lambda}^2 = \lambda^2 D/\nu^3$ which does not depend on the scaling exponents,

$$\frac{d\bar{\lambda}}{d\ell} = \frac{2-d}{2}\bar{\lambda} + K_d \frac{2d-3}{4d}\bar{\lambda}^3. \tag{A3}$$

The KPZ fixed point $\bar{\lambda}^*_{\mathrm{KPZ}}$ is then defined by the nonzero solutions of $d\bar{\lambda}/d\ell = 0$. This means that the asymptotic description of the system is given by the equation

$$\frac{\partial h}{\partial t} = \nabla^2 h + \frac{\bar{\lambda}^*_{\mathrm{KPZ}}}{2}(\nabla h)^2 + \xi \tag{A4}$$

with

$$\langle \xi(\mathbf{x},t)\xi(\mathbf{x}',t')\rangle = 2\delta^d(\mathbf{x}-\mathbf{x}')\delta(t-t'), \tag{A5}$$

where we have used the knowledge that $\bar{\lambda}$ involves a specific combination of coefficients. Thus, within the domain of attraction of the KPZ fixed point, the asymptotic behavior of any Eq. (A1) is that of the fixed point Eq. (A4). In the present case, this point might seem somewhat trivial because the only nonuniversal feature of Eq. (A1) lies in the arbitrariness of the relative magnitudes of the coefficients. But note that, in general, the microscopic equation associated with a given atomistic model will involve additional terms which are irrelevant in the RG sense.

In order to characterize the scaling behavior associated with the KPZ fixed point (and to discover whether there is scaling behavior in the first place), we need to consider the RG equations for the coefficients in Eq. (A1)

$$\frac{d\nu}{d\ell} = \left(z - 2 + \frac{2-d}{4d}K_d\bar{\lambda}^2\right)\nu, \tag{A6}$$

$$\frac{d\lambda}{d\ell} = (z+\alpha-2)\lambda, \tag{A7}$$

$$\frac{dD}{d\ell} = \left(z - d - 2\alpha + K_d\frac{\bar{\lambda}^2}{4}\right)D. \tag{A8}$$

For the fixed point Eq. (A4), we know that, by definition, the coefficients do not change under a change in scale. Thus, choosing the initial conditions

$$(\nu(\ell=0),\lambda(\ell=0),D(\ell=0)) = (1,\bar{\lambda}^*_{\mathrm{KPZ}},1), \tag{A9}$$

we must have

$$\left.\frac{d\nu}{d\ell}\right|_{\bar{\lambda}=\bar{\lambda}^*_{\mathrm{KPZ}}} = \left.\frac{d\lambda}{d\ell}\right|_{\bar{\lambda}=\bar{\lambda}^*_{\mathrm{KPZ}}} = \left.\frac{dD}{d\ell}\right|_{\bar{\lambda}=\bar{\lambda}^*_{\mathrm{KPZ}}} = 0, \tag{A10}$$

which can only be ensured by fixing the values of z and α. But note that within the domain of attraction of the KPZ fixed point, which follows from Eq. (A3), the behavior of *any* equation asymptotically reduces to that of Eq. (A4) and, thus, the scaling behavior obtained from Eq. (A10). The scaling behavior associated with other fixed points of the RG and more complicated parameter spaces is determined following similar logic.

[1] Alvin L.-S. Chua, C. A. Haselwandter, C. Baggio, and D. D. Vvedensky, Phys. Rev. E **72**, 051103 (2005).
[2] C. A. Haselwandter and D. D. Vvedensky, Phys. Rev. Lett. **98**, 046102 (2007).
[3] C. A. Haselwandter and D. D. Vvedensky, EPL **77**, 38004 (2007).
[4] C. A. Haselwandter and D. D. Vvedensky, Phys. Rev. E **76**, 041115 (2007).
[5] C. A. Haselwandter and D. D. Vvedensky, Phys. Rev. E **77**, 061129 (2008).
[6] S.-K. Ma and G. F. Mazenko, Phys. Rev. B **11**, 4077 (1975).
[7] T. S. Chang, D. D. Vvedensky, and J. F. Nicoll, Phys. Rep. **217**, 279 (1992).
[8] A.-L. Barabási and H. E. Stanley, *Fractal Concepts in Surface Growth* (Cambridge University Press, Cambridge, England, 1995).
[9] T. Halpin-Healy and Y.-C. Zhang, Phys. Rep. **254**, 215 (1995).
[10] C. A. Haselwandter and D. D. Vvedensky, Int. J. Mod. Phys. B **22**, 3721 (2008).
[11] S. Clarke and D. D. Vvedensky, Phys. Rev. Lett. **58**, 2235 (1987).
[12] A. Madhukar and S. V. Ghaisas, CRC Crit. Rev. Solid State Mater. Sci. **14**, 1 (1988).
[13] H. Metiu, Y.-T. Lu, and Z. Y. Zhang, Science **255**, 1088 (1992).
[14] T. Shitara, D. D. Vvedensky, M. R. Wilby, J. Zhang, J. H. Neave, and B. A. Joyce, Phys. Rev. B **46**, 6815 (1992).
[15] T. Shitara, D. D. Vvedensky, M. R. Wilby, J. Zhang, J. H. Neave, and B. A. Joyce, Phys. Rev. B **46**, 6825 (1992).
[16] J. W. Evans, P. A. Thiel, and M. C. Bartelt, Surf. Sci. Rep. **61**, 1 (2006).
[17] P. Šmilauer and D. D. Vvedensky, Phys. Rev. B **52**, 14263 (1995).
[18] J. Villain, J. Phys. I **1**, 19 (1991).
[19] Z.-W. Lai and S. Das Sarma, Phys. Rev. Lett. **66**, 2348 (1991).
[20] C. Ratsch, A. Zangwill, P. Šmilauer, and D. D. Vvedensky, Phys. Rev. Lett. **72**, 3194 (1994).
[21] L.-H. Tang and T. Nattermann, Phys. Rev. Lett. **66**, 2899 (1991).
[22] Here, we are disregarding special cases such as the possibility

that no fixed point is approached asymptotically (Ref. [2]).
[23] C. Herring, in *The Physics of Powder Metallurgy*, edited by W. E. Kingston (McGraw-Hill, New York, 1951), pp. 143–179.
[24] W. W. Mullins, J. Appl. Phys. **28**, 333 (1957).
[25] T. Sun, H. Guo, and M. Grant, Phys. Rev. A **40**, 6763 (1989).
[26] C. Ratsch, M. F. Gyure, S. Chen, M. Kang, and D. D. Vvedensky, Phys. Rev. B **61**, R10598 (2000).
[27] S.-J. Yu, Y.-J. Zhang, Q.-L. Ye, P.-G. Cai, X.-W. Tang, and G.-X. Ye, Phys. Rev. B **68**, 193403 (2003).
[28] Z.-N. Fang, B. Yang, M.-G. Chen, C.-H. Zhang, J.-P. Xie, and G.-X. Ye, Thin Solid Films **517**, 3408 (2009).
[29] M. Itoh, G. R. Bell, A. R. Avery, T. S. Jones, B. A. Joyce, and D. D. Vvedensky, Phys. Rev. Lett. **81**, 633 (1998).
[30] M. Kotrla and P. Šmilauer, Phys. Rev. B **53**, 13777 (1996).
[31] L. Pauling, J. Am. Chem. Soc. **69**, 542 (1947).
[32] H.-C. Kan, S. Shah, T. Tadyyon-Eslami, and R. J. Phaneuf, Phys. Rev. Lett. **92**, 146101 (2004).
[33] H.-C. Kan, R. Ankam, S. Shah, K. M. Micholsky, T. Tadayyon-Eslami, L. Calhoun, and R. J. Phaneuf, Phys. Rev. B **73**, 195410 (2006).
[34] T. Tadayyon-Eslami, H.-C. Kan, L. C. Calhoun, and R. J. Phaneuf, Phys. Rev. Lett. **97**, 126101 (2006).
[35] E. Medina, T. Hwa, M. Kardar, and Y.-C. Zhang, Phys. Rev. A **39**, 3053 (1989).
[36] M. F. Gyure, J. J. Zinck, C. Ratsch, and D. D. Vvedensky, Phys. Rev. Lett. **81**, 4931 (1998).
[37] J. Krug and M. Rost, Phys. Rev. B **60**, R16334 (1999).
[38] G. Hu, G. Orkoulas, and P. D. Christofides, Chem. Eng. Sci. **64**, 3668 (2009).
[39] G. Hu, G. Orkoulas, and P. D. Christofides, Ind. Eng. Chem. Res. **48**, 6690 (2009).
[40] M. Kardar, G. Parisi, and Y.-C. Zhang, Phys. Rev. Lett. **56**, 889 (1986).